IEEE Access
Multidisciplinary | Rapid Review | Open Access Journal

Date of publication xxxx 00, 0000, date of current version xxxx 00, 0000.

Digital Object Identifier 10.1109/ACCESS.2017.Doi Number

Hybrid Wind/PV/Battery Energy Management-Based Intelligent Non-Integer Control for Smart DC-Microgrid of Smart University

Ahmad Aziz Al Alahmadi[1], Youcef Belkhier[2], Nasim Ullah[1], (Member, IEEE), Habti Abeida[1], Mohamed S. Soliman[1,3], (Senior Member, IEEE), Yahya Salameh Hassan Khraisat[1,4], and Yasser Mohammed Alharbi[1]

[1]Department of Electrical Engineering, College of Engineering, Taif University KSA, P. O. Box 11099, Taif, 21944, Saudi Arabia
[2]Laboratoire de Technologie Industrielle et de l'Information (LTII), Faculté de Technologie, Université de Bejaia, Bejaia 06000, Algeria
[3]Department of Electrical Engineering, Faculty of Energy Engineering, Aswan University, Aswan 81528, Egypt.
[4]Department of Electrical and Electronics Engineering, Al-Balqa' Applied University, Amman 19117, Jordan.

Corresponding author: Youcef Belkhier (e-mail: youcef.belkhier@univ-bejaia.dz).

This work was supported by the Research Groups Program funded by Deanship of Scientific Research, Taif University, Ministry of Education, Saudi Arabia, under Grant 1-440-6140.

ABSTRACT Global environmental changes, nuclear power risks, losses in the electricity grid, and rising energy costs are increasing the desire to rely on more renewable energy for electricity generation. Recently, most people prefer to live and work in smart places like smart cities and smart universities which integrating smart grid systems. The large part of these smart grid systems is based on hybrid energy sources which make the energy management a challenging task. Thus, the design of an intelligent energy management controller is required. The present paper proposes an intelligent energy management controller based on combined fuzzy logic and fractional-order proportional-integral-derivative (FO-PID) controller methods for a smart DC-microgrid. The hybrid energy sources integrated into the DC-microgrid are constituted by a battery bank, wind energy, and photovoltaic (PV) energy source. The source-side converters (SSCs) are controller by the new intelligent fractional order PID strategy to extract the maximum power from the renewable energy sources (wind and PV) and improve the power quality supplied to the DC-microgrid. To make the microgrid as cost-effective, the (wind and PV) energy sources are prioritized. The proposed controller ensures smooth output power and service continuity. Simulation results of the proposed control schema under Matlab/Simulink are presented and compared with the super twisting fractional-order controller.

INDEX TERMS Renewable Energy, Smart University, DC-Microgrid, Energy Management control, Fuzzy logic control, Fractional order control

I. INTRODUCTION

The production of electrical energy in the world generates various types of pollution. Thermal power plants (coal, oil) are responsible for atmospheric emissions linked to the combustion of fossil fuels. On the other hand, nuclear power plants, whose development intensified following the oil crisis, have not had a negative impact on air quality. On the other hand, they produce radioactive waste which causes major problems in terms of storage, processing, and transport. Today, the fear of using only one energy source with all its risks, and the opening of the electricity production market are all factors that give renewable energies (hydraulic, wind, solar, biomass, etc.) an important place in electricity production [1], [2].

The demand for energy by consumers is generally not evenly distributed over time and problems of the phasing of energy produced versus energy consumed arise. The stability of the grid depends on the balance between production and consumption [3]. The increase in the penetration rate of renewable energies will therefore be conditioned by their participation in these different services, which will be favored by the association with these clean energy sources, of electrical energy storage systems [4]. Storage is therefore the key to the penetration of these energies in the electricity grid. Not only does it provide a technical solution for the grid

This article has been accepted for publication in a future issue of this journal, but has not been fully edited. Content may change prior to final publication. Citation information: DOI 10.1109/ACCESS.2021.3095973, IEEE Access

Nomenclature and Abbreviations

PV, WT	Photovoltaic and Wind turbine	V_w, V_{pv}, V_b,	wind voltage input of the rectified, PV voltage, battery voltage, V
PMSG	Permanent Magnet Synchronous Generator	V_g,	AC grid voltage,
BSS	Battery Storage System	V_L	load voltage
SSCs	Source-Side Converters	V_{dc}, $V_{dc\text{-}ref}$	direct voltage in the DC grid and its reference respectively, Volts
LSCs	Load-Side Converters	I_d, I_q and V_d, V_q	current and voltage components along d and q rotor axes respectively, A and Volts
EMU	Energy Management Unit	E	electromotive force corresponding to the open circuit battery voltage, Volts
AC	Alternative Current	Q	battery capacity
MPPT	Maximum Power Point Tracking	p	pair pole number of the PMSG
SOC,	battery State Of Charge	R_s	stator phase resistances, Ω
SOC_{max},	battery State Of Charge minimum value		
SOC_{min}	battery State Of Charge maximum value		
A	area swept by the rotor blades, m^2	i_w, i_{pv}, i_b, i_g, i_L	wind current rectified, PV current, battery current, AC grid current rectified, and load current, A
T_{em}	PMSG electromagnetic torque, N.m	I_{bat}	battery charging current
P_{Load}	load powers, Watt	ρ	air density, kg/m^3
$P_{Battery}$	battery power		
P_w, P_{pv}	aerodynamic power and PV power respectively, Watt	λ	tip speed ratio
P_{AC}, P_g	exchanged powers between the proposed system and the AC grid, before and after the local variable AC load, respectively, Watt	ψ_d, ψ_q, ψ_f	rotor flux components along d and q rotor axes and rotor flux, Wb

operator to ensure a real-time balance of production and consumption, but it also enables the best possible use of renewable resources by avoiding load shedding in the event of overproduction. Combined with local renewable generation, decentralized storage would also have the advantage of improving the robustness of the electricity network by allowing islanding of the area supplied by this resource. Also, a well-placed energy storage system (ESS) increases the quality of the power supplied by providing better control of frequency and voltage and reduces the impact of its variability by adding value to the current supplied, especially if the electricity is delivered during peak periods [5], [6].

The integration of renewable energies together with the energy storage system in a standalone micro grid is an emerging research area. Generally, it is preferred to integrate different renewable energies such as tidal, wind, and PV to yields a positive impact on the maximum capacity of the energy storage system. Usually, ESS is constituted by a combination of a battery and supercapacitors, which helps extend battery life-time and offers a fast system response to compensate the transients [7]. However, loads are necessary when all (energy sources and battery storage systems (BSS)) are connected; thus, the AC grid is used instead of supercapacitors [8]. A micro grid is classified into DC, AC, or a combination of both types. Compared with AC microgrid, DC microgrid shows several benefits such as fewer parameters to control, facilitate integration, and simple structure. On the other hand, AC type needs more information like the synchronization of the frequency and reactive power, which makes the control design process a challenging task. Moreover, a DC micro grid offers the possibility to work in different modes like AC microgrid, standalone, or integrated with the AC microgrid [9], [10].

Due to the latest development in power electronics, the autonomous DC microgrid can work at its maximum performance. However, because of the renewable energy sources stochastic nature, the smooth operation and continuous power transmission to the loads need a supplementary energy management unit. Numerous research works on the energy management control dedicated to AC microgrids can be found in the literature, but given the important differences between the AC and DC microgrid dynamics, these control strategies can not be adopted for DC microgrids. In fact, in the standard design of the DC microgrid, the load converters and the energy sources are parallelly connected where the energy is consumed or supplied through the DC-link. Thus, the control of the DC-link voltage is needed for an efficient and stable operation of the DC microgrid [11]-[12]. Several control strategies have appeared in the literature to address the issues of the DC-link voltage. In [13], a review of the recent trends and development in hybrid micro grid topology with energy resource planning and control is presented. In [14], a combined fuzzy controller and voltage control are proposed to regulate the DC voltage. In [15], a fuzzy logic control strategy with reduced rules is investigated. In [16], a dual proportional-integral controller is adopted. However, the aforementioned control strategies are linear and can regulate the DC-link in a small operating interval. Thus, to overcome this restriction, nonlinear controls have been investigated in the literature. in [17], an adaptive droop controller algorithm is proposed. Energy management-based optimal control is investigated in [18] for multiple energy storage system in a microgrid. In [19], robust H∞ control strategy is developed.

This article has been accepted for publication in a future issue of this journal, but has not been fully edited. Content may change prior to final publication. Citation information: DOI 10.1109/ACCESS.2021.3095973, IEEE Access

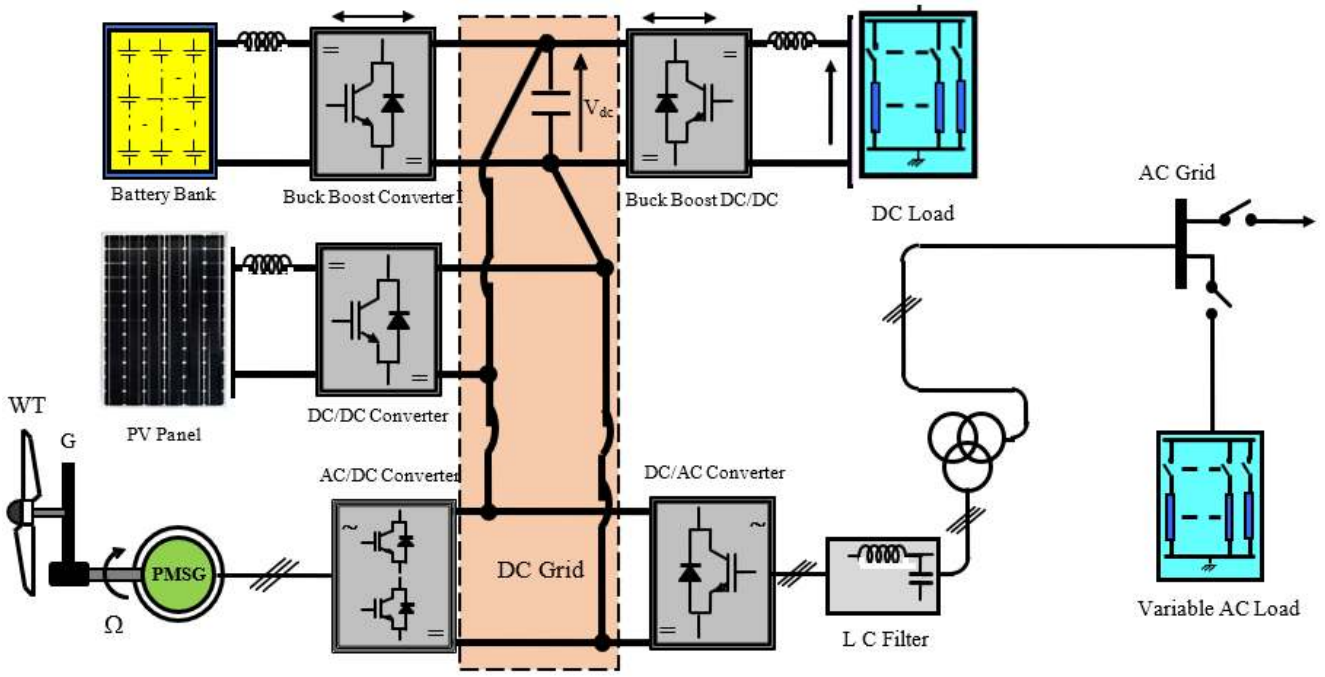

FIGURE 1. **Studied hybrid System Structure**

Robust sliding mode strategy is proposed in [20]. In [21], an adaptive backstepping control method is designed. A Lyapunov-based strategy is presented in [22]. Feedback linearization control is discussed in [23]. A hybrid combined backstepping and sliding mode controller is investigated in [24]. However, the previous proposed nonlinear controls show limitations in performances in the case of droop control strategy and optimal energy management has given the multiple integrated energy storage system, poor stability for the H∞ method, chattering issues concerning the sliding mode. Also, the major part of these controls highly depends on fixed gains which are very sensitive to parameter uncertainties and external disturbances. Finally, the last part represents the energy management unit.

In the same context, in the present work, a new fractional order PID controller is proposed combined with a fuzzy logic method to address the problems faced by the conventional integer controls in hybrid energy management. Fractional-order controllers offer additional advantages over integer order controls such as robust behavior to oscillations and the measurement noise and high degree of freedom. The proposed new controller is integrated with an energy management unit for a DC-microgrid integrated with several stochastic sources and essential DC loads illustrated by Figure 1. The proposed intelligent Fractional-Order PID (IFO-PID) controls will be used as a low-level controller, when the energy management unit serves as high-level controller which generates appropriate references for the IFO-PID and monitors the generated and consumed power.

This paper addresses the following two main objectives: controlling the source-side converters (SSCs) to extract the maximum power from the renewable energy sources (wind and PV) using the proposed IFO-PID. The second task is to improve the power quality supplied to the DC-microgrid by regulating the reactive power and the DC-link voltage to their references using the energy management unit (EMU).

The novelty and contribution of the present work are summarized as follows:

- The new fractional order PID (FO-PID) controller combined with a fuzzy logic strategy is developed for a DC-microgrid integrated with several stochastic sources and essential DC loads.
- The fuzzy logic method is selected as a fuzzy gain supervisor to adaptively adjust gains of the FO-PID which greatly enhances the robustness of the proposed approach against various uncertainties external disturbances.
- The essential characteristic of this approach is the extremely reduced number of the fixed gains used by the proposed strategy which avoids its sensitivity to parameter uncertainties, which highly improves the robustness property and global stability of the system.
- The global stability of the system and is ensured and further validated by extensive simulation results.

The present work is organized such as the mathematical description of the hybrid energy system is given in section 2. Section 3 deals with the design of the proposed hybrid controller strategy. In section 4, the numerical results are

This article has been accepted for publication in a future issue of this journal, but has not been fully edited. Content may change prior to final publication. Citation information: DOI 10.1109/ACCESS.2021.3095973, IEEE Access

presented and discussed. Finally, the main conclusions and future works are established in section 5.

II. MATHEMATICAL DESCRIPTION OF THE HYBRID ENERGY SYSTEM

The studied hybrid energy system integrated smart DC-microgrid is illustrated by Figure 1, where three main parts can be distinguished: the hybrid energy sources constituted by the wind energy, solar energy, and the battery storage systems connected to the DC-link through their respective converters. The second part represents the loads assumed to be a priority which in the case of a smart university may include laboratory experimentation benches, fans, and lighting. A maximum power point tracking algorithm is used on both the wind and solar (PV) conversion systems to force them to operate at maximum power. The energy management unit computes the total consumed and produced energy to select the adequate control modes.

A. WIND SYSTEM MODEL

The mathematical model of the wind power that can be transformed by the turbine is given by [25]:

$$P_m = \frac{1}{2}\rho C_p(\beta,\lambda)Av^3 \tag{1}$$

$$T_m = \frac{P_m}{\omega_t} \tag{2}$$

$$C_p(\beta,\lambda) = \frac{1}{2}\left(\frac{116}{\lambda_i} - 0.4\beta - 5\right)e^{-\left(\frac{21}{\lambda_i}\right)} \tag{3}$$

$$\lambda_i^{-1} = \left(\lambda + 0.08\beta\right)^{-1} - 0.035\left(1+\beta^3\right)^{-1} \tag{4}$$

$$\lambda = \frac{\omega_t R}{v} \quad , \tag{5}$$

where, v denotes the wind speed, β represents the pitch angle, ω_t denotes the turbine speed, R represents the blades radius, C_p denotes the power coefficient, λ denotes the tip-speed ratio, ρ denotes the water density, and A represents the area of the blades. The wind conversion system is based on a permanent magnet synchronous generator (PSMG) which is expressed as [25]:

$$v_{dq} = R_{dq}i_{dq} + L_{dq}\dot{i}_{dq} + \psi_{dq}p\omega_m \tag{6}$$

$$J\dot{\omega}_m = T_m - T_e - f_{fv}\omega_m \tag{7}$$

$$T_e = \frac{2}{3}p\psi_{dq}^T i_{dq} \tag{8}$$

where, $i_{dq} = \begin{bmatrix} i_d \\ i_q \end{bmatrix}$ represents the stator current vector, T_e represents the electromagnetic torque, f_{fv} represents the viscous friction coefficient, $L_{dq} = \begin{bmatrix} L_d & 0 \\ 0 & L_q \end{bmatrix}$ represents dq inductances matrix, J is the moment of inertia, $\psi_{dq} = \begin{bmatrix} \psi_f \\ 0 \end{bmatrix}$ represents the flux linkages vector, $v_{dq} = \begin{bmatrix} v_d \\ v_q \end{bmatrix}$ represents voltage stator vector, and $R_{dq} = \begin{bmatrix} R_s & 0 \\ 0 & R_s \end{bmatrix}$ represents the stator resistance matrix. . To design the proposed control method, the model of the SCCs needs to be expressed. Thus, the model of the wind source converter (see Figure 2) is given as [26], [27]:

$$\frac{dV_w}{dt} = \frac{I_w}{C_w} - \frac{I_{Lw}}{C_w} \tag{9}$$

$$\frac{V_w}{L_w} = \frac{dI_w}{dt} + (1-U_1)\frac{V_{dc}}{L_w} - D_1 \tag{10}$$

$$\frac{dV_{dc}}{dt} = (1-U_1)\frac{I_{Lw}}{C_{dc}} - \frac{I_{Ow}}{C_{dc}} + D_2 \tag{11}$$

where, I_w denotes the wind current rectified, L_w denotes the inductance, I_{Lw} denotes the current of the inductor, V_w denotes the voltage input rectified, U_1 denotes the control signal, V_{dc} denotes the link voltage, D_1 and D_2 denotes dynamics uncertainty in the energy stage parameters. Depending on the state of the storage system, which it will be discussed in the energy management section, the wind system can be operated under MPPT for maximum power extraction or off-MPPT for power balance as shown in Fig. 2. The MPPT algorithm is detailed in the flowchart of Fig. 3.

In case of power generation excess and no storage capacity in the battery system, the proposed energy management unit (EMU) switches the wind controller from the MPPT mode to the off-MPPT mode in order to reduce the generated power and maintain a balanced power in the standalone system. In off-MPPT, the voltage reference is carried out as [23]:

$$V_{ref} = \frac{P_L - P_w}{I_w} \tag{12}$$

where, P_L is the load power and P_w is the power from the wind energy system.

B. SOLAR POWER SYSTEM MODEL

The solar conversion system (SCS) is constituted by the PV panel connected to the DC-link through a DC-DC boost converter. The SCS mathematical model is given as below:

This article has been accepted for publication in a future issue of this journal, but has not been fully edited. Content may change prior to final publication. Citation information: DOI 10.1109/ACCESS.2021.3095973, IEEE Access

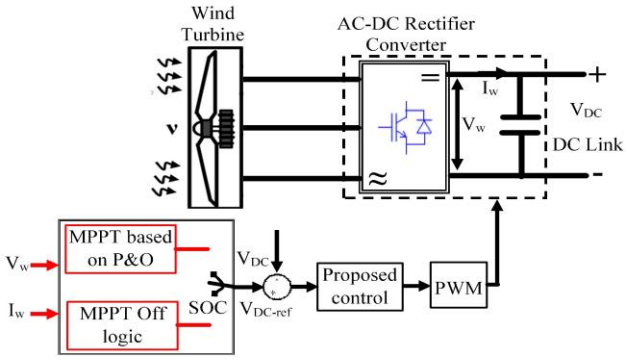

FIGURE 2. **Wind energy system with controller.**

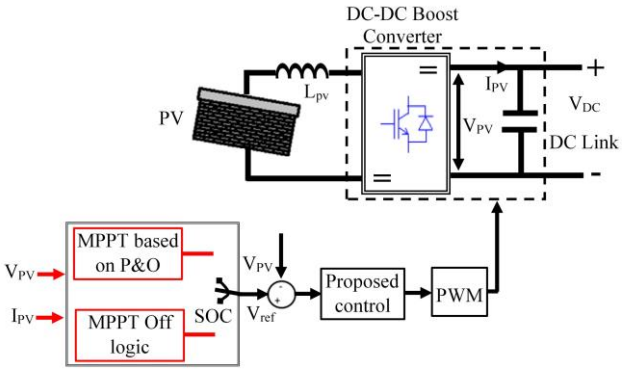

FIGURE 4. **Solar energy system with controller.**

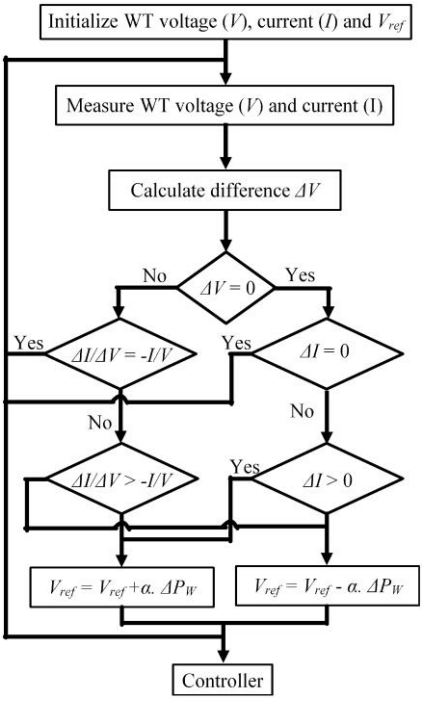

FIGURE 3. **MPPT Algorithm of the wind system.**

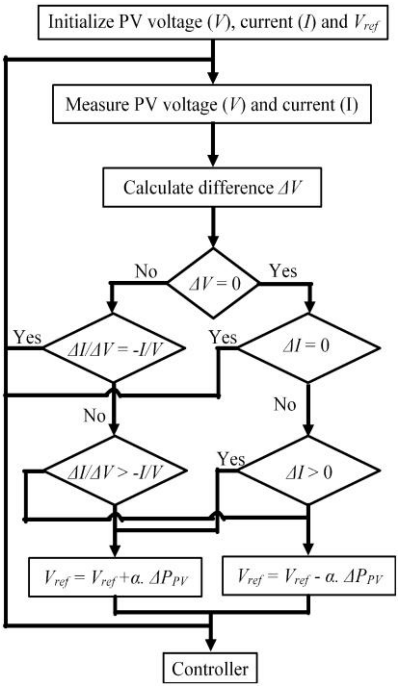

FIGURE 5. **MPPT algorithm of the solar energy system.**

$$\frac{dV_{pv}}{dt} = \frac{I_{pv}}{C_{pv}} - \frac{I_{Lpv}}{C_{pv}} \tag{13}$$

$$\frac{V_{pv}}{L_{pv}} = \frac{dI_{pv}}{dt} + (1 - U_2)\frac{V_{dc}}{L_{pv}} - D_3 \tag{14}$$

$$\frac{dV_{dc}}{dt} = (1 - U_2)\frac{I_{Lpv}}{C_{dc}} - \frac{I_{Opv}}{C_{dc}} + D_4 \tag{15}$$

where, I_{pv} denotes the PV current, L_{pv} denotes the inductance, V_{pv} denotes the voltage of the PV panel, L_{Lpv} denotes the current of the inductor, U_2 denotes the control signal, D_3 and D_4 denotes dynamics uncertainty in the energy stage parameters as given by Figure 3. Here also, according to the state of the storage system, the PV conversion system can be operated under MPPT for maximum power extraction or off-MPPT for power balance as shown in Figs. 4 and 5. Furthermore, in case of power generation excess and no storage capacity in the battery system, the proposed energy management system switches the PV controller from the MPPT mode to the off-MPPT mode in order to reduce the generated power and maintain a balanced power in the standalone system. In off-MPPT, the voltage reference is carried out as [23]:

$$V_{ref} = \frac{P_L - P_{pv}}{I_{pv}} \tag{16}$$

where, P_L is the load power and P_{pv} is the power from the PV panel energy system.

C. BATTERY SYSTEM MODEL

This article has been accepted for publication in a future issue of this journal, but has not been fully edited. Content may change prior to final publication. Citation information: DOI 10.1109/ACCESS.2021.3095973, IEEE Access

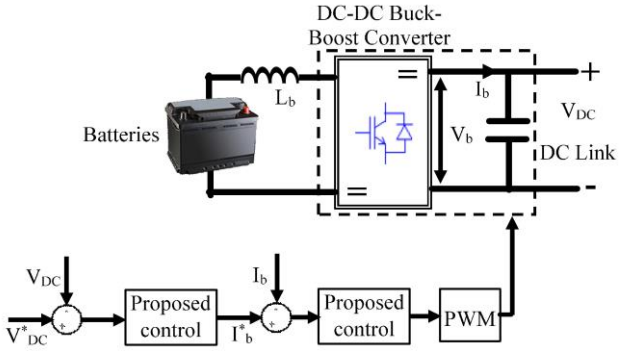

FIGURE 6. Battery storage system with controller.

In this application, a standard battery is connected to the DC-link through a bidirectional DC-DC back-boost converter connected at the DC-link of the microgrid (see Figure 6). The role of this converter is to maintain the DC-link voltage constant despite the power changes in the sources and the load. The DC-link voltage is regulated at it references to compute the reference current of the battery and then design the voltage controller through the proposed strategy as shown in Fig. 6. The Battery State of Charge (SOC) model is modelled as described below [26]:

$$SOC = 100\left(1 + \frac{\int I_{bat}\,dt}{Q}\right) \tag{17}$$

The SOC, the amount of electricity stored during the charge, is an important parameter to be controlled. The battery SOC must detect by the proposed supervisory system to make decisions according to its status and the required power. In a battery, the ampere-hours stored during a time t corresponds to a nominal capacity Q and a charging current I_{bat}. The battery charge-discharge depends on the available power, the demand and the SOC. The energy constraints of the battery are determined based on the SOC limits:

$$SOC_{\min} \le SOC \le SOC_{\max} \tag{18}$$

where, SOCmin and SOCmax are the minimum and the maximum allowable states for the battery safety. The model of the BSS converter is given as:

$$\frac{V_b}{L_b} = \frac{dI_b}{dt} + U_3\frac{V_{dc}}{L_b} - D_5 \tag{19}$$

$$\frac{dV_{dc}}{dt} = U_3\frac{I_b}{C_{dc}} - \frac{I_{Ob}}{C_{dc}} + D_6 \tag{20}$$

Where, I_b denotes the current of the battery, V_b denotes the voltage of the battery, U_3 denotes the controller signal, D_5 and D_6 denotes dynamics uncertainty in the energy stage parameters. The maximum power allowed during the charge/discharge of the battery system is fixed to 6525 Watts during the charge phase and to 10440 Watts during the discharge phase, according to the parameters of the battery storage system given by ref [27].

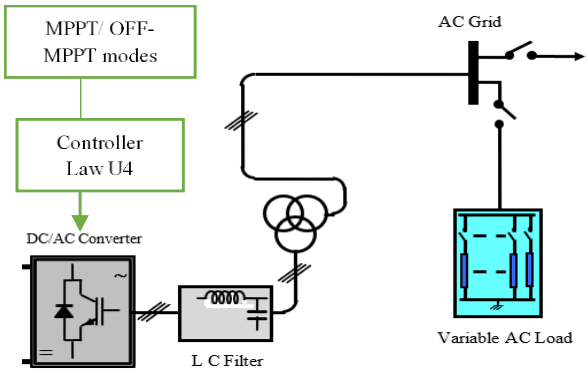

FIGURE 7. AC Load system.

D. AC GRID MODEL

Similar wind and AC grid converters are used which is a buck-to-buck converter (see Figure 7). Then, the mathematical modeling of the AC grid converter system can be expressed as given below:

$$\frac{dV_g}{dt} = \frac{I_g}{C_g} - \frac{I_{Lg}}{C_g} \tag{21}$$

$$\frac{V_g}{L_g} = \frac{dI_g}{dt} + (1-U_4)\frac{V_{dc}}{L_g} - D_7 \tag{22}$$

$$\frac{dV_{dc}}{dt} = (1-U_4)\frac{I_{Lg}}{C_{dc}} - \frac{I_{Og}}{C_{dc}} + D_8 \tag{23}$$

where, I_g denotes the rectified current of the grid, V_g denotes the voltage input rectified of the grid to the boost converter, U_4 denotes the controller signal, D_7 and D_8 denotes dynamics uncertainty in the energy stage parameters, L_{Lg} denotes the current of the inductor, and C_{dc} denotes the DC-link capacitor. From the model (9)-(15) and model (21)-(23), a generalized compact form can be deduced as given below:

$$\frac{dV_j}{dt} = \frac{I_j}{C_j} - \frac{I_{Lj}}{C_j} \tag{24}$$

$$\frac{V_j}{L_j} = \frac{dI_j}{dt} + (1-U_i)\frac{V_{dc}}{L_j} - D_i \tag{25}$$

$$\frac{dV_{dc}}{dt} = (1-U_i)\frac{I_{Lj}}{C_{dc}} - \frac{I_{Oj}}{C_{dc}} + D_{i+1} \tag{26}$$

Where, the subscript j denotes the given sub-terms w, pv, b, and g of each converter. The subscript i denotes 1 in case of wind, 2 in case of PV, 3 in case of Battery, and 4 in case of AC grid.

This article has been accepted for publication in a future issue of this journal, but has not been fully edited. Content may change prior to final publication. Citation information: DOI 10.1109/ACCESS.2021.3095973, IEEE Access

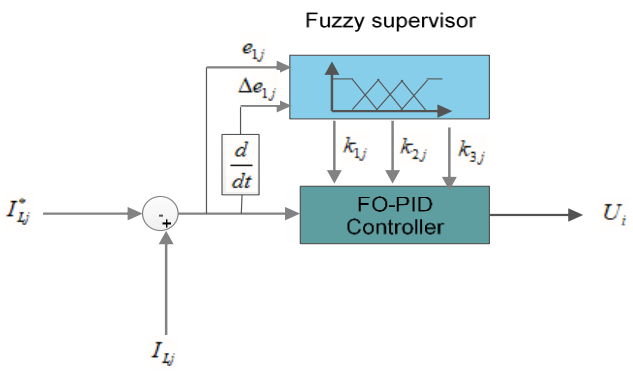

FIGURE 8. SSCs controller law computation with the IFO-PID.

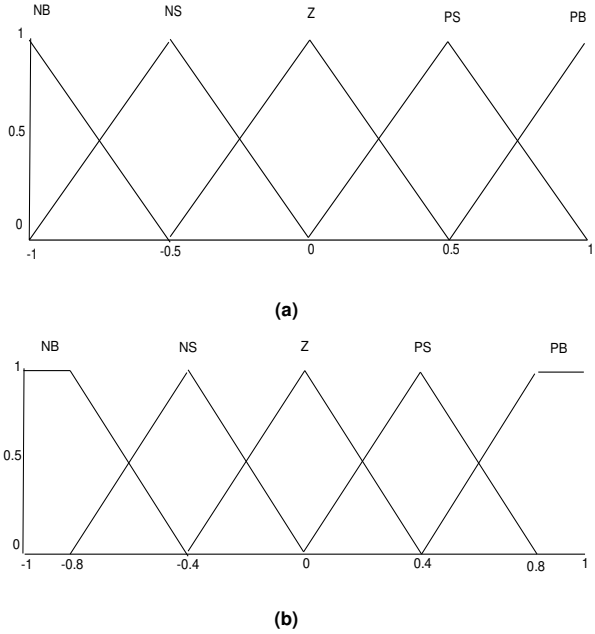

FIGURE 9. The fuzzy controller configuration. (a) Input membership function, (d) Output membership function

Remark1: It should be remaindered that in the present work the MPPT algorithm is only used on SSCs, thus the supply of the grid energy is assumed to be constant.

E. LOAD SIDE CONVERTERS (LSCs) MODEL

In Figure 1 it can be seen that a parallel DC-DC buck converter is used to connect the DC priority loads which their power loads are constant. These parallel converters are adopted to minimize the converters' stress and divide the load. The mathematical model of several parallel converters is given as below:

$$\frac{U_p V_{dc}}{L_p} = \frac{dI_{Lp}}{dt} + \frac{V_{Loadp}}{L_p} - D_{I_{Lp}} \tag{27}$$

$$\frac{dV_{Loadp}}{dt} = \frac{I_{Lp}}{C_p} - \frac{V_{Loadp}}{R_{Lp}C_c} + D_{V_{Loadp}} \tag{28}$$

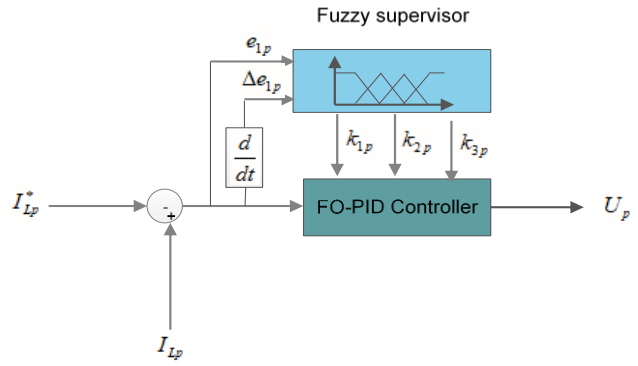

FIGURE 10. SSCs controller law computation with the IFO-PID.

where, U_p denotes the control law, L_{Lp} denotes the current of the inductor, V_{Loadp} denotes the load voltage, $D_{V_{Loadp}}$ denotes dynamics uncertainty of the voltage, and $D_{I_{Lp}}$ denotes dynamics uncertainty in the current.

III. PROPOSED CONTROLLER DESIGN PROCESS

The purpose of the proposed intelligent fractional-PID order is to compute the SCCs controller law shown in the generalized model (24)-(26) represented by U_i and to compute the LSCs controller law shown in the generalized model (27)-(28) represented by U_p as illustrated by Figures 1-5.

Two steps are needed to design the proposed IFO-PID: first, the controller laws are calculated by the FO-PID and then, the fixed gains are adopted by the Fuzzy gain supervisor, which makes the proposed controller adaptive and robust against parameter uncertainties. In [26], a proportional-integral (PI) control is proposed to compute the controllers of the source-side converters and load-side converters. However, it is well known that fixed gains are very difficult to calculate under parameter uncertainties or variations [27]. Thus, the IFO-PID controller is introduced to improve the robustness and resolve the problems faced by the PI loops.

A. SSCs CONTROLLERS DESIGN

To compute the SSCs controller law U_i, the following Lyapunov function as:

$$V_{j1} = 0.5e_j^2 \tag{29}$$

Where, $e_j = C_j(V_j - V_j^*)$ is the voltage error and V_j^* denotes the desired voltage controller. From (24) and the derivative of e_j it yields:

$$e_j = I_j - I_{Lj} - C_j\dot{V}_j^* \tag{30}$$

This article has been accepted for publication in a future issue of this journal, but has not been fully edited. Content may change prior to final publication. Citation information: DOI 10.1109/ACCESS.2021.3095973, IEEE Access

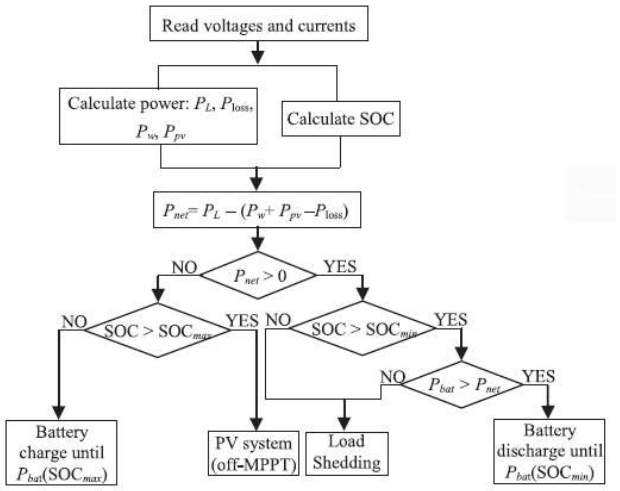

FIGURE 11. **Energy management system.**

To design the voltage controller, the desired current I_{Lj}^{*} is needed which is deduced from (30) as given below:

$$I_{Lj}^{*} = I_j - C_j \dot{V}_j^{*} + k_j e_j \tag{31}$$

From Eq. (31) derivative of (29), it gives:

$$\dot{V}_{j1} = -k_j e_j^2 \tag{32}$$

Where, $k_j > 0$ is the gain matrix. The BSS desired current is generated by the energy management unit. Thus, to design the controller law U_i, the fractional order-PID (FO-PID) control is adopted as illustrated in Fig. 8. For more information about the FO-PID control, the reader is referred to [27] and [28]. The expression of the controller law U_i is given as:

$$U_i = k_{1j} e_{1j} + k_{2j} e_{1j} D_t^{-\alpha} + k_{3j} e_{1j} D_t^{\beta} \tag{33}$$

Where, k_{1j}, k_{2j}, and k_{3j} denotes the gain matrix, $D_t^{-\alpha}$ represents order α of fractional integration and D_t^{β} represents the order β of differentiation, and e_{1j} denotes the current error expressed as:

$$e_{1j} = (I_{Lj} - I_{Lj}^{*}) \tag{34}$$

Where, the desired current I_{Lj}^{*} in Eq. (31) is computed using the FO-PID as below:

$$I_{Lj}^{*} = k_{1j} e_{2j} + k_{2j} e_{2j} D_t^{-\alpha} + k_{3j} e_{2j} D_t^{\beta} \tag{35}$$

Where, e_{2j} denotes the DC-link voltage error expressed as:

$$e_{2j} = (V_{dc} - V_{dc}^{*}) \tag{36}$$

However, as mentioned previously fixed gains are very

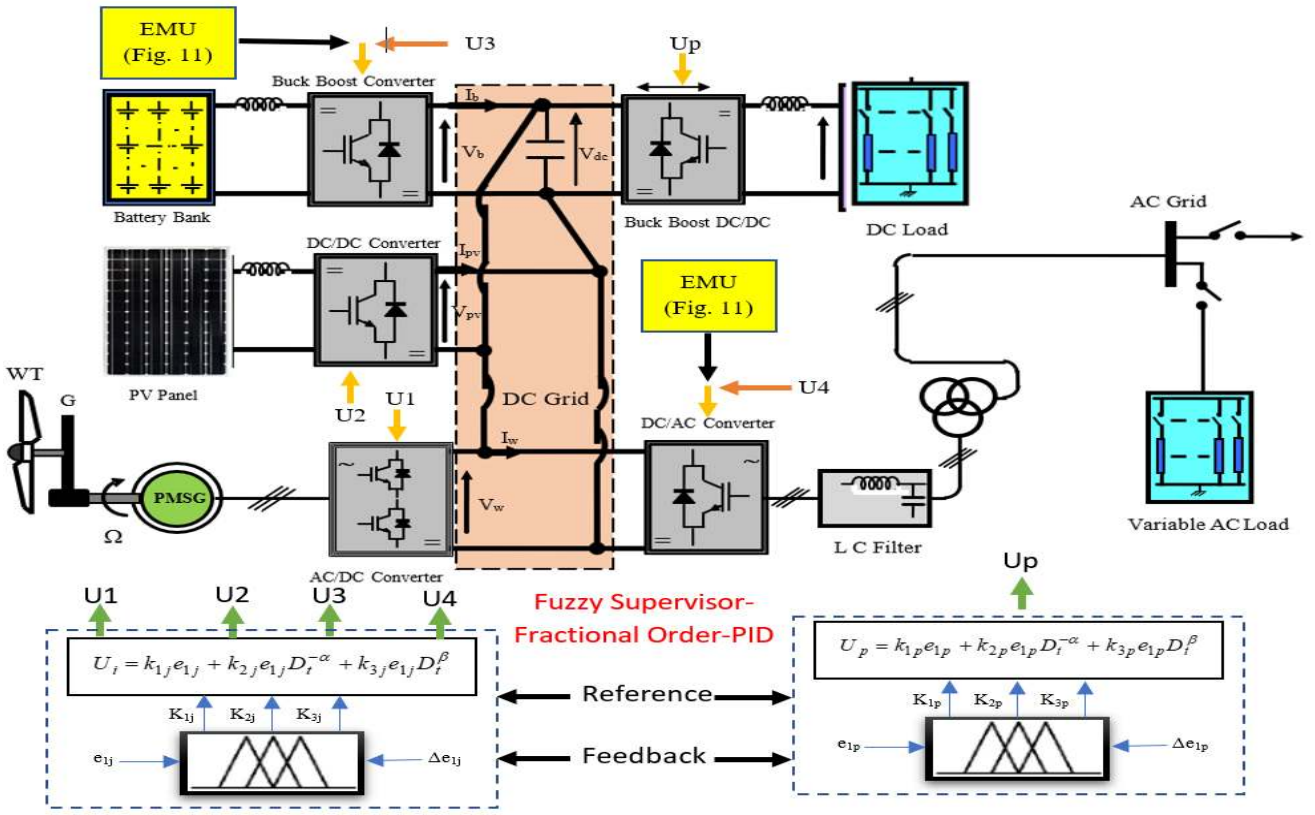

FIGURE 12. **Proposed controller Structure**

This article has been accepted for publication in a future issue of this journal, but has not been fully edited. Content may change prior to final publication. Citation information: DOI 10.1109/ACCESS.2021.3095973, IEEE Access

sensitive to parameter changes. Thus, the fuzzy method is selected as fuzzy supervisor is used for the adaptation of the gains k_{1j}, k_{2j}, and k_{3j} thus, it solves the problem caused by imprecise parameters. The fuzzy inputs are chosen as the current error in the case of the controller law computation given by Eq. (33) and its derivative or the DC-link error in the case of the desired current given by Eq. (35) and its derivative. Triangular and trapezoidal types symmetrical and uniformly distributed are used to select the membership functions as given in Fig. 9. The method of partitioning these functions is given according to Lee and Yubazaki [29] and [30]. Their method is based on the idea of sharing the same parameter by several membership functions. The advantage of this method is that the number of parameters of the membership functions is significantly reduced. The decision-making output is obtained using a Max-Min fuzzy inference where the crisp outputs are calculated by the center of gravity defuzzification method. In Table 1, the linguistic variables corresponding to the inputs-outputs of the fuzzy gain scheduling are chosen as: Negative Big (NB), Negative Small (NS), Zero (Z), Positive Big (PB), and Positive Small (PS) [29].

Table 1: Fuzzy logic rules of the SSCs and LSCs

$e_{j,p}$ \ $\Delta e_{j,p}$	NB	NS	Z	PS	PB
NB	NB	NB	NS	NS	Z
NS	NB	NB	NS	Z	PS
Z	NS	NS	Z	PS	PS
PS	NS	Z	PS	PB	PB
PB	Z	PS	PS	PB	PB

Remark 2: the fuzzy logic controller chosen to compute the gains of the fractional order-PID controller is justified by the fact that fixed gains are complicated to calculate when the system is exposed to parameter changes. Also, the stability and robustness proof of the fractional order are clearly demonstrated in [27] and [38], thus they are not considered in the present work.

B. LSCs CONTROLLER DESIGN

The expression of the controller law U_p is given as (see Fig. 10):

$$U_p = k_{1p}e_{1p} + k_{2p}e_{1p}D_t^{-\alpha} + k_{3p}e_{1p}D_t^{\beta} \tag{37}$$

Where, k_{1p}, k_{2p}, and k_{3p} denotes the gain matrix, and e_{1p} denotes the current error expressed as:

$$e_{1p} = (I_{Lp} - I_{Lp}^{*}) \tag{38}$$

Where, the desired current I_{Lp}^{*} in Eq. (38) is computed using the FO-PID as below:

$$I_{Lp}^{*} = k_{1p}e_{2p} + k_{2p}e_{2p}D_t^{-\alpha} + k_{3p}e_{2p}D_t^{\beta} \tag{39}$$

Where, e_{2p} denotes the load voltage error expressed as:

$$e_{2p} = (V_{Loadp} - V_{Loadp}^{*}) \tag{40}$$

C. ENERGY MANAGEMENT UNIT (EMU)

The energy management unit aim is to coordinate and control all the operations in the microgrid system. From Figs. 2-7, it can be seen that the energy management unit described by the MPPT Mode/of-MPPT mode algorithm is used to generate the references of the SSCs and load-side converters controller law. The energy management unit generates the references based on the measured input power available and the consumed for both the SSCs and LSCs. The renewable sources are prioritized as mentioned previously on the loads.

The BSS works in charge/discharge mode and regulates the DC-link voltage at its reference value. The power in the microgrid is balanced under different power generation forms oh the renewable sources and the load demand condition. When the source-side converters generate abundant power, the supply power is used to charge the battery storage system. In case the power generated by the source-side converters is not enough, the power in the AC grid is used to supply the loads as shown in Fig. 1. The mathematical model of the power balance is given as [17], [26]:

$$P_W + P_{pv} + P_g = P_{Load} + P_{Battery} \tag{41}$$

This article has been accepted for publication in a future issue of this journal, but has not been fully edited. Content may change prior to final publication. Citation information: DOI 10.1109/ACCESS.2021.3095973, IEEE Access

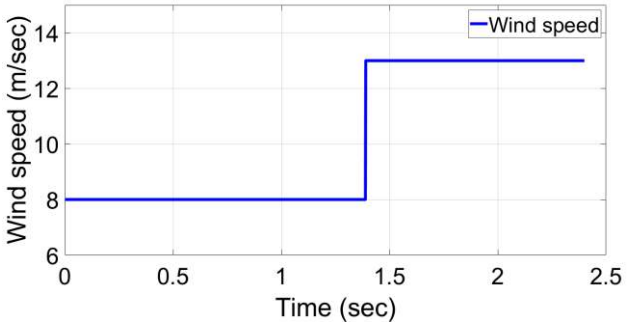

FIGURE 13 Wind speed

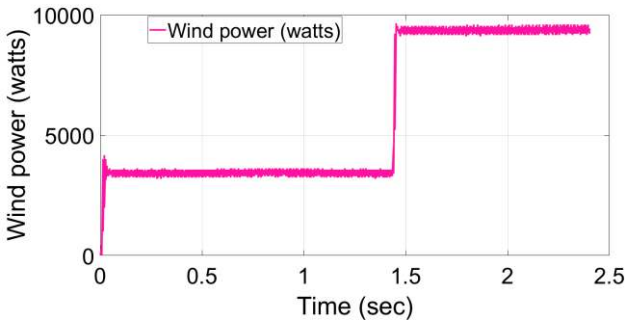

FIGURE 14 Wind power

According to Fig. 11, four modes of the energy management unit can be distinguished and each mode depends on two conditions: the battery state and the generated power. When the generated power from the renewable energies is more than the load demand, the additional power is transferred to charge the battery to its $SOC_{\max}$, at this limit the MPPT is switched to off-mode. In case the generated power cannot meet the load demand, the required power is supplied by the battery storage system until $SOC_{\min}$, and in case the power generated by the source-side converters is not enough, the power in AC grid is used to supply the loads. Thus, the generalized energy management controller structure is illustrated in Fig. 12.

VI. NUMERICAL RESULTS

The present paper proposed a combined hybrid energy system integrated smart DC-microgrid is illustrated by Fig. 1, where three main parts can be distinguished: the hybrid energy sources constituted by the wind energy, solar energy, and the BSS connected to the DC-link through their respective converters. The second part represents the loads assumed to be a priority which in the case of a smart university may include laboratory experimentation benches, fans, and lighting. A maximum power point tracking algorithm is used on both the wind and solar (PV) conversion systems to force them to operate at maximum power. The energy management unit computes the total consumed and

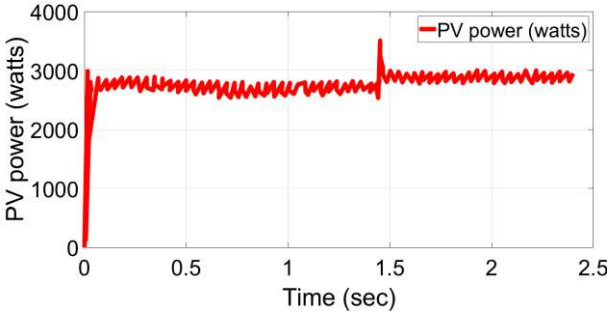

FIGURE 15 Solar power

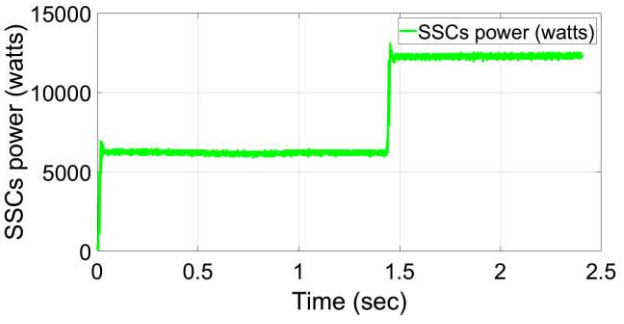

FIGURE 16 SSCs power

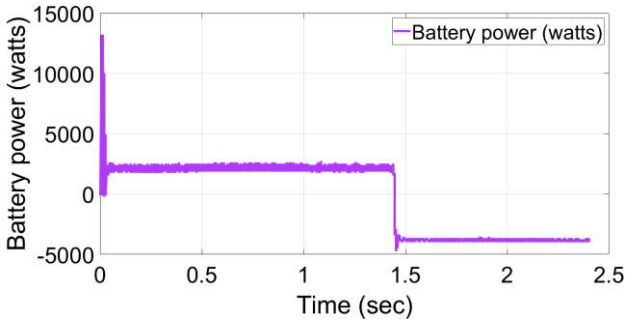

FIGURE 17 BSS power

produced energy to order to select the adequate control modes.

The simulation results of the proposed system are performed under Matlab/Simulink and the used parameters can be found in [27]. The DC-link reference value is fixed to 240 V. The simulation test is focused on the energy management unit performances illustrated in Fig. 11. Firstly, the DC load of 8000 watts is connected to the DC-link through two load-side converters when the battery storage system state of charge (SOC) is initially at 80 %. Fig. 13, shows the wind profile between 8-13m/s. Fig. 14 shows the generated wind power which is varying between 4000 and 10000 watts) according to the wind speed. A 3000 watts PV power is generated as shown in Fig. 15 under a radiance of 600 watts/m2 and a temperature of 25°C. Fig. 16, depict the generated power P_{dg} from both PV and wind sources. According to the present response, the generated power P_{dg} varies between 7000 and 13000 watts.

This article has been accepted for publication in a future issue of this journal, but has not been fully edited. Content may change prior to final publication. Citation information: DOI 10.1109/ACCESS.2021.3095973, IEEE Access

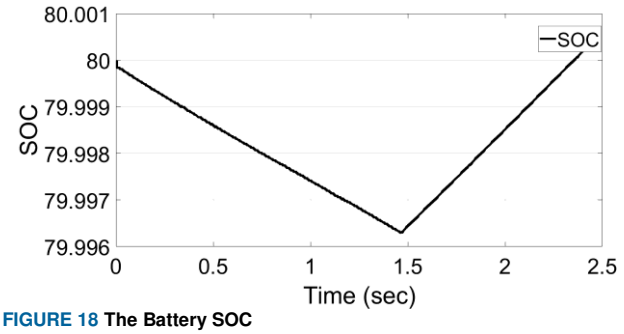

FIGURE 18 The Battery SOC

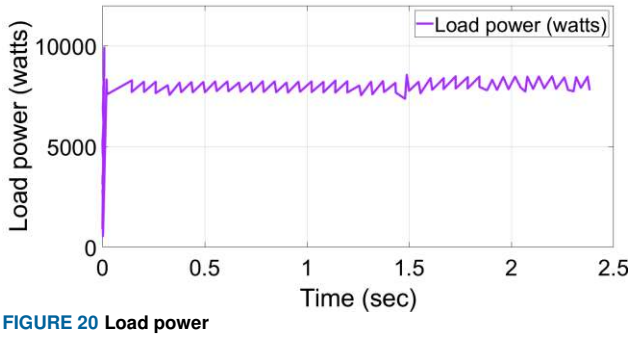

FIGURE 20 Load power

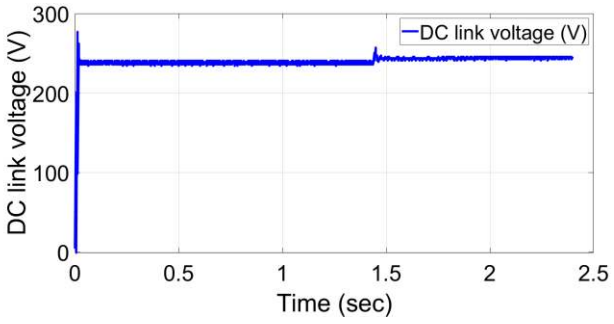

FIGURE 19 DC-link voltage

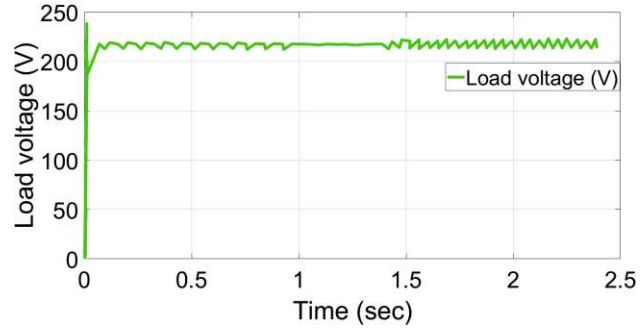

FIGURE 21 Load voltage

Figs. 17 and 18 show the battery power and its SOC. From the presented results, the battery supplies the microgrid with about 2300 watts in the time intervals [0-1.4] *s* when *SOC* > 20%, while in the time intervals [1.4- 2.3] *s* the generated P_{dg} is more than the load power. Thus, the battery is charged with about 4500 watts from the microgrid. Fig. 19, shows the DC-link voltage of both the SSCs and LSCs for the PI and proposed IFO-PID, where it can be seen that both regulate the DC-link at its reference value. However, the proposed IFO-PID shows superior performances in terms of the steady-state error and the convergence criterion. Fig. 20 shows that the proposed energy management control transmits a constant power to the loads, about 8300 watts. Fig. 21 clearly indicate that the proposed IFO-PID regulate the output voltage at its refence (220V).

A comparative analysis with previous works has been performed in the present section to highlight the advantages

Table 2: Comparative analysis of the proposed strategy with recent references

Ref.	Microgrid elements	Method	Main contribution	The novelty of the proposed strategy
[14]	Wind-PV+BSS+ DC loads (Houses)	Distribution Voltage Control	FLC + Gain scheduling	*A new adaptive and intelligent controller is proposed. The controller is used to control both SSCs and LSCs contrary. *The number of the fixed gains used by the proposed strategy is the extremely reduced (Zero fixed gains) as all the gains are computed by the fuzzy supervisor which avoid its sensitivity to parameter uncertainties, and thus, highly improve the robustness property and global stability of the system. *Increases the power produced.
[15]	PV-Wind-BSS-Residence	Energy Management	Two low-complexity FLC	
[16]	PV-Wind-BSS-SOFC-Loads	Coordinated control	Two Feed-Back control loops and Feed-Forward control loop	
[17]	PV-BBSS-Loads	Energy Management	adaptive droop control	
[21]	PV-Wind Generator-BSS-Loads	Energy Management	Adaptive Backstepping	
[27]	PV-Wind-BSS-Load	Energy Management+ SSCs control	Super Twisting Fractional Order	
Proposed strategy	Wind-PV-BSS-Loads	Energy management + SSCs Control	Fuzzy Supervisory-Fractional Order-PID control	

This article has been accepted for publication in a future issue of this journal, but has not been fully edited. Content may change prior to final publication. Citation information: DOI 10.1109/ACCESS.2021.3095973, IEEE Access

Table 3: Results comparison of the proposed strategy with that of ref. [27], FO-PID and PID

Controller	Proposed IFO-PID	Super Twisting Factional Order [27]	FO-PID	PID
Wind power (W)	9800 (+3.15%)	9500	9800	9400
PV power (W)	3000 (+50%)	2000	3000	1900
SSCs power (W)	13000 (+4%)	12500	13000	12300
BSS power stored (W)	2500 (+13.64%)	2200	2500	2100
BSS power supplied (W)	4500 (+12.5%)	4000	4500	4000
Load power (W)	8300 (+2.5%)	8100	8300	8000
Complexity	Low	High	Low	Very Low
Robustness	High (Zero fixed gains)	Poor (more than 7 fixed gains)	Low (more than 5 fixed gains)	Very poor (more than 10 fixed gains)
Performance	Very High	High	High	Low

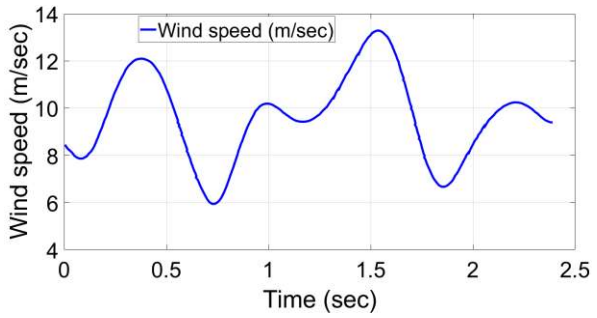

FIGURE 22. Random wind speed

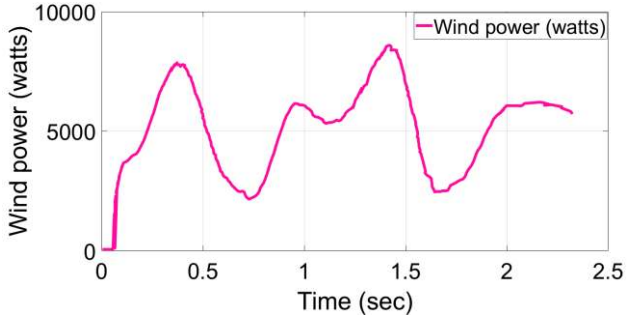

FIGURE 23. Wind power under random wind speed

of the proposed IFO-PID. The comparative analysis is shown by Table 2. Extensive comparative analysis with ref. [27], FO-PID and PID is demonstrated in Table 3, where it can be seen that the proposed strategy generates more power and show high performance over the compared control strategies. From the present comparative analysis, the proposed controller produces +3.15% wind power, +50% PV power, +2.5% load power over the super twisting fractional-order and more when compared to the PID control.

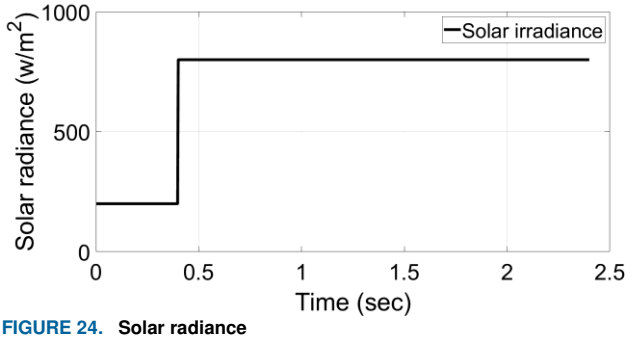

FIGURE 24. Solar radiance

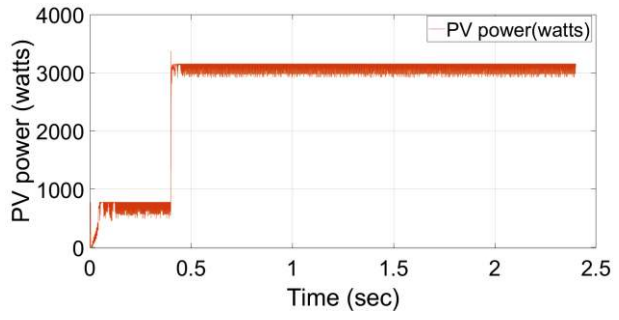

FIGURE 25. Solar power under random solar radiance

In summary, the proposed control strategy has well managed the hybrid energy, and well achieved the objectives of the present work, and shows higher performances when compared to the other methods.

To test the robustness of the proposed energy management strategy, a random variation of the wind speed and solar radiance is used as shown by Fig. 22 and Fig. 23 respectively. Fig. 24 shows the wind power generated under random wind profile. The wind system appears to work at MPPT based on the reported results. Figure 25 clearly

This article has been accepted for publication in a future issue of this journal, but has not been fully edited. Content may change prior to final publication. Citation information: DOI 10.1109/ACCESS.2021.3095973, IEEE Access

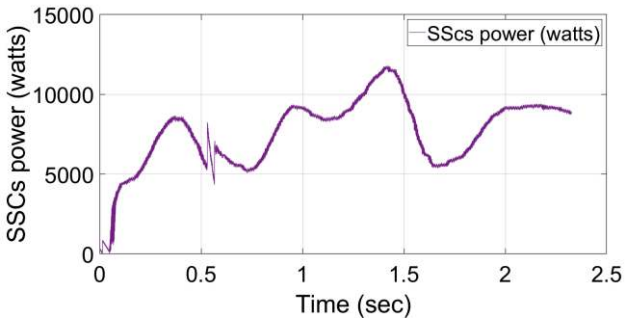

FIGURE 26. SSCs power under random variations.

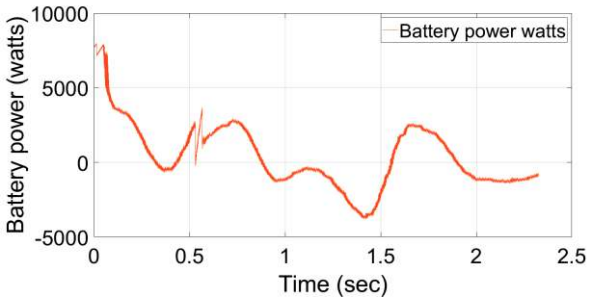

FIGURE 27. BSS power under random variations.

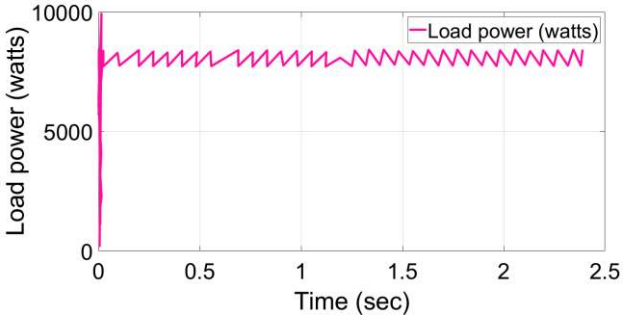

FIGURE 28. Load power under random variations

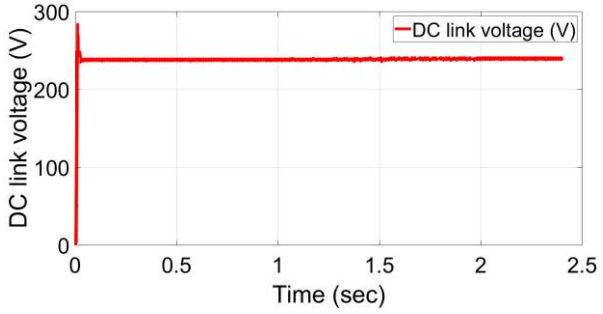

FIGURE 29 DC-link voltage under random variations

demonstrates how the MPPT control (see Fig. 5) forces the PV panel to extract the maximum power regardless of solar radiation variations. Fig. 26 shows the power generated from both PV and wind sources. From the given results, it can be seen that the power generated is maintained between 5000-13000W which is the same as in the first test (see Fig. 16). Fig. 27 shows the BSS power under the random variations which is varying between 5000 and -5000W. The BSS works perfectly in charge/discharge mode. Fig. 28 depict that the proposed energy management control transmits a constant power to the load, about 8300W, here also it's the same as in the first case (see Fig. 20). Finally, Fig. 29 shows the DC-link voltage response. It is clear from the reported response that the proposed technique effectively regulates the DC voltage at its reference. Thus, the proposed energy management strategy well validates the objectives even under random variations, ensures smooth output power and service continuity.

V. CONCLUSION

In this paper, a novel intelligent fractional order PID controller is proposed for the Energy management of hybrid energy sources contacted to a smart grid through a DC-link voltage. The hybrid energy sources integrated to the DC-microgrid are constituted by a battery bank, wind energy, and photovoltaic (PV) energy source. The source side converters (SCCs) are controller by the new intelligent fractional order PID strategy to extract the maximum power from the renewable energy sources (wind and PV) and improve the power quality supplied to the DC-microgrid. To make the microgrid as cost-effective, the (Wind and PV) energy sources are prioritized. The proposed controller ensures smooth output power and service continuity. Simulation results of the proposed control schema under Matlab/Simulink are presented and compared with the other nonlinear controls. Extensive comparative analysis with super twisting fractional order control, FO-PID and PID is demonstrated in Table 3, where it can be seen that the proposed strategy generates more power and show high performance over the proposed control strategies. From the present comparative analysis, the proposed controller produces +3.15% wind power, +50% PV power, +2.5% load power over the super twisting fractional-order and more when compared to the PID control. Future works will be focused on the experimental validation of the proposed control with a real test bench.

REFERENCES

[1] H. Dinf, J. Yun, D. M. Kim, K. H. Lee, K. Kim, "A Home Energy Management System with Renewable Energy and Energy Storage Utilizing Main Grid and Electricity Selling," *IEEE Access*, vol. *8*, pp. 49436-49450, 2020.

[2] C. Byer, A. Botterud, "Additional Capacity Value from Synergy of Variable Renewable Energy and Energy Storage," *IEEE Transactions on Sustainable Energy,* vol. 11, no. 2, pp. 1106-1109, 2020.

[3] M. Rizwan, L. Hong, W. Muhammad, S. W. Azeem, Y. Li, "Hybrid Harris Hawks optimizer for integration of renewable energy sources considering stochastic behavior of energy sources," *Int Trans Electr Energ Syst.,* 2021. DOI:31/e12694.

[4] Y. Sun, Z. Zhao, M. Yang, D. Jia, W. Pei, B. Xu, "Overview of Energy Storage in Renewable Energy Power Fluctuation Mitigation," *CSEE Journal of Power and Energy Systems*, vol. 6, no. 1, pp. 160-173, 2020.

[5] T. Salameh, M. A. Abdelkareem, A. G. Olabi, E. T. Sayed, M. Al-Chaderchi, H. Rezk, "Integrated standalone hybrid solar PV, fuel cell and diesel generator power system for battery or supercapacitor storage systems in Khorfakkan, United Arab Emirates," *International Journal of Hydrogen Energy*, vol. 46, no. 8, pp. 6014-6027, 2021.

[6] M. Çolak, I. Kaya, "Multi-criteria evaluation of energy storage technologies based on hesitant fuzzy information: A case study for Turkey," *Journal of Energy Storage*, vol. 28, pp. 101211, 2021.

[7] M. A. Hannan, M. M. Hoque, A. Mohamed, A. Ayob, "Review of energy storage systems for electric vehicle applications: Issues and challenges," *Renewable and Sustainable Energy Reviews*, vol. 69, pp. 771-789, 2017.

[8] R. Amirante, E. Cassone, E. Distaso, P. Tamburrano, "Overview of recent developments in energy storage: Mechanical, electrochemical and hydrogen technologies," *Energy Conversion and Management*, vol. 132, pp. 372-387, 2017.

[9] T. Ma, H. Yang, L. Lu, "Development of hybrid battery-supercapacitor energy storage for remote area renewable energy systems," *Appl. Energy*, vol. 153, pp. 56–62, 2017.

[10] X. Wang, D. Yu, S. Blond, Z. Zhao, P. Wilson, "A novel controller of a battery-supercapacitor hybrid energy storage system for domestic applications," *Energy and Buildings*, vol. 141, pp. 167-174, 2017.

[11] A. Kadri, H. Marzougui, A. Aouiti, F. Bacha, "Energy management and control strategy for a DFIG wind turbine/fuel cell hybrid system with super capacitor storage system," *Energy*, vol. 192, pp. 116518, 2020.

[12] A. K. Barik, D.C. Das, A. Latif, S. M. S. Hussain, T. S. Ustun, " Optimal Voltage–Frequency Regulation in Distributed Sustainable Energy-Based Hybrid Microgrids with Integrated Resource Planning," *Energies,* vol. 14, pp. 2735, 2021. https://doi.org/10.3390/en14102735.

[13] A. K. Barik, S. Jaiswal, D.C. Das, "Recent trends and development in hybrid microgrid: a review on energy resource planning and control," *International Journal of Sustainable Energy*, 2021. DOI: 10.1080/14786451.2021.1910698.

[14] H. Kakigano, Y. Miura, and T. Ise, "Distribution voltage control for DC microgrids using fuzzy control and gain-scheduling technique," *IEEE Trans. Power Electron.*, vol. 28, no. 5, pp. 2246-2258, May 2013.

[15] D. A. Aviles, J. Pascual, F. Guinjoan, G. G. Gutierrez, R. G. Orguera, J. L. Proano, P. Sanchis, T. E. Motoasca. An Energy Management System Design Using Fuzzy Logic Control: Smoothing the Grid Power Profile of a Residential Electro-Thermal Microgrid. *IEEE Access*, vol. 9, pp. 25172-25188, 2021.

[16] M. Kumar, S. C. Srivastava, and S. N. Singh, ``Control strategies of a DC microgrid for grid connected and islanded operations," *IEEE Trans. Smart Grid*, vol. 6, no. 4, pp. 1588-1601, Jul. 2015.

[17] H. Hajebrahimim, S. M. Kaviri, S. Eren, A. Bakhshai. A New Energy Management Control Method for Energy Storage Systems in Microgrids. *IEEE Transactions on Power Electronics*, Vol. 35, no. 11, pp. 11612-11624, 2020.

[18] Xu Y, Shen X. (2018). Optimal Control Based Energy Management of Multiple Energy Storage Systems in a Microgrid. *IEEE Access*, 6, 32925-32934.

[19] A.-R.-I. Mohamed, H. H. Zeineldin, M. M. A. Salama, and R. Seethapathy, ``Seamless formation and robust control of distributed generation microgrids via direct voltage control and optimized dynamic power sharing," *IEEE Trans. Power Electron.*, vol. 27, no. 3, pp. 1283_1294, Mar. 2012.

[20] B. A. M. Trevino, A. El Aroudi, E. V. Idiarte, A. C. Pastor, R. M. Salamero, "Sliding-mode control of a boost converter under constant power loading conditions," *IET Power Electronics*, vol. 12, no. 3, pp. 521-529, 2019.

[21] T. K. Roy, M. A. Mahmud, A. M. T. Oo, M. E. Haque, K. M. Muttaqi, and N. Mendis, ``Nonlinear adaptive backstepping controller design for islanded DC microgrids," *IEEE Trans. Ind. Appl.*, vol. 54, no. 3, pp. 2857-2873, May 2018.

[22] Nami A., A. Iovine, M. J. Carrizosa, G. Damm, and P. Alou, ``Nonlinear control for DC microgrids enabling ef_cient renewable power integration and ancillary services for AC grids," *IEEE Trans. Power Syst.*, vol. 34, no. 6, pp. 5136-5146, Nov. 2019.

[23] X. Li, X. Zhang, W. Jiang, J. Wang, P. Wang, X. Wu, "A Novel Assorted Nonlinear Stabilizer for DC–DC Multilevel Boost Converter with Constant Power Load in DC Microgrid," *IEEE Trans. Power Electron.,* vol. 35, no. 10, pp. 11181-11192, 2020.

[24] J. Wu, Y. Lu. Adaptive Backstepping Sliding Mode Control for Boost Converter With Constant Power Load. *IEEE Access*, vol. 7, pp. 50797-50807, 2019.

[25] S. Tamalouzt. Performances of direct reactive power control technique applied to three level-inverter under random behavior of wind speed. *Rev. Roum. Sci. Techn. – Electrotechn. et Energ*., vol. 64, no. 1, pp. 33–38, 2019.

[26] P. S. Kumar, R. P. S. Chandrasena, V. Ramu, G. N. Srinivas, K. V. S. M. Babu, "Energy management system for small scale hybrid wind solar battery based microgrid," *IEEE Access*, vol. 8, pp. 8336-8344, 2020.

[27] Y. M. Alharbi, A. A. Al Alahmadi, N. Ullah, H. Abeida, M. S. Soliman, Y. S. H. Khraisat, "Super Twisting Fractional Order Energy Management Control for a Smart University System Integrated DC Micro-Grid," *IEEE Access*, Vol. 8, pp. 128692-128704, 2020.

[28] I. Sami, S. Ullah, Z. Ali, N. Ullah, J. S. Ro, "A super twisting fractional order terminal sliding mode control for DFIG-based wind energy conversion system," *Energies*, vol. 13, pp. 2158, 2020.

[29] M. A. Lee, H. Takagi, "Dynamic control of genetic algorithms using fuzzy logic techniques," *Proceedings of International conference on Genetic Algorithms*, San Mateo, CA, pp. 76–83, 1993.

[30] N. Yubazaki, M. Otami, T. Ashid, K. Hirota, "Dynamic fuzzy control method and its application to positioning of induction motor," *Proceedings of Fourth IEEE International Conference on Fuzzy Systems*, Japan, pp. 1095–1102, 1995.